LBL-18996
Preprint c.2

Lawrence Berkeley Laboratory

UNIVERSITY OF CALIFORNIA

RECEIVED
LAWRENCE
BERKELEY LABORATORY
JAN 14 1986
LIBRARY AND
DOCUMENTS SECTION

Materials & Molecular Research Division

Submitted to Metallurgical Transactions

MATRIX AND INTERFACIAL PRECIPITATION
IN THE W-Ni-Fe SYSTEM

J.B. Posthill and D.V. Edmonds

November 1985

TWO-WEEK LOAN COPY
This is a Library Circulating Copy
which may be borrowed for two weeks.

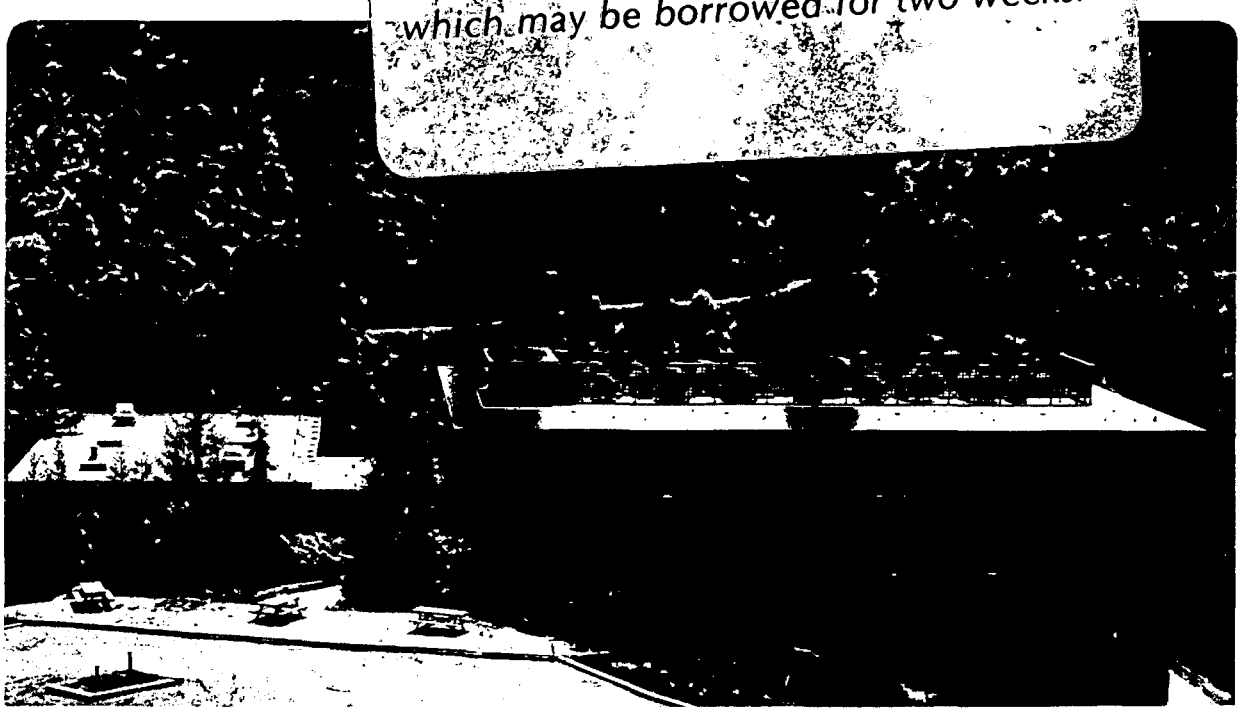

LBL-18996 c.2

Prepared for the U.S. Department of Energy under Contract DE-AC03-76SF00098

DISCLAIMER

This document was prepared as an account of work sponsored by the United States Government. While this document is believed to contain correct information, neither the United States Government nor any agency thereof, nor the Regents of the University of California, nor any of their employees, makes any warranty, express or implied, or assumes any legal responsibility for the accuracy, completeness, or usefulness of any information, apparatus, product, or process disclosed, or represents that its use would not infringe privately owned rights. Reference herein to any specific commercial product, process, or service by its trade name, trademark, manufacturer, or otherwise, does not necessarily constitute or imply its endorsement, recommendation, or favoring by the United States Government or any agency thereof, or the Regents of the University of California. The views and opinions of authors expressed herein do not necessarily state or reflect those of the United States Government or any agency thereof or the Regents of the University of California.

Matrix and Interfacial Precipitation in the W-Ni-Fe System

J.B. Posthill* and D.V. Edmonds**

*National Center for Electron Microscopy
Materials and Molecular Research Division
Lawrence Berkeley Laboratory
University of California
Berkeley, CA 94720

**Department of Metallurgy and Science of Materials
University of Oxford
Parks Road
Oxford OX1 3PH

Abstract

The microstructural changes of a commercial 90W-5Ni-5Fe heavy alloy as a function of thermal treatment have been examined using a variety of metallographic techniques. Upon solution treating at 1350°C for 1 hour, quenching, and subsequently aging at 750 - 850°C for various times, a discontinuous precipitation reaction was observed in the matrix phase. Concurrently, precipitation of a face-centered cubic phase with lattice parameter, a_0 = 1.096 $\pm$ 0.004 nm occurred at the interphase boundaries between tungsten grains and matrix. Metallographic examination of two specially manufactured "matrix-composition" alloys, which have been heat treated in a similar manner, provided additional information concerning these respective precipitation reactions. The products of the discontinuous reaction were found to be tungsten and solute-depleted matrix phase in both the heavy alloy and a matrix-composition alloy. Moreover, an M_6C eta-carbide (M = Ni, Fe and W) obtained in a second matrix-composition alloy was found to have the same crystal structure as the interfacial phase in the heavy alloy which is believed to be an $M_{12}C$ eta-carbide in agreement with previous results[1].

1. Introduction

Tungsten heavy alloys have received considerable attention since 1935 when McLennan and Smithells[2] first reported the development of a 90W-10(Ni,Cu) alloy. More generally, the tungsten heavy alloys are a group of materials based on 80 - 97 wt % tungsten and produced by liquid-phase sintering in the presence of nickel and other element(s) (e.g., Cu, Fe, Cr). Sintering in the temperature range 1440 - 1500°C allows the non-tungsten elements to melt whilst simultaneously dissolving some of the tungsten. The presence of nickel ensures that the liquid phase will sufficiently wet the solid tungsten particles thereby enabling consolidation to occur at a temperature far below the melting point of tungsten (T_m=3410° C). Normally, this process is carried out in a reducing atmosphere and densities >99% of the theoretical density are routinely obtained.

The resulting microstructure of a W-Ni-Fe heavy alloy consists of a contiguous network of spheroidal tungsten-rich b.c.c. grains (∿20-30 μm diameter) embedded in a Ni-Fe-W face-centered cubic matrix (γ-phase). This structure is responsible for an interesting and technologically important combination of properties, viz., high density (16 - 18.5 g-cm^{-3}), high tensile strength (800 - 1200 N-mm^{-2}), and good tensile elongation (10 - 30%). Tungsten heavy alloys can certainly find application wherever a high density material is needed, and when high strength and adequate ductility are also required they become even more attractive.

Previous metallographic work has concentrated on those features of the microstructure thought to be most responsible for maintaining good mechanical properties. The effects of certain microstructural variables such as the size[3] and contiguity[4,5,6] of tungsten grains, porosity[7] and

matrix volume fraction[4,6,8,9] have been addressed. The influence of varying the nickel:iron ratio on the microstructure and mechanical properties of W-Ni-Fe heavy alloys has also been explored.[10,11,12] The application of high resolution microanalytical techniques has allowed detailed studies of hydrogen embrittlement[13] and impurity element segregation.[6,14,15] Additionally, certain precipitation reactions have been investigated including precipitation hardening of the W-phase,[16,17] W-W grain boundary precipitation,[18] W-γ interphase boundary precipitation[1,11,19,20,21] and precipitation within the matrix region[11,19,21,22]. The present contribution is concerned with clarifying the nature of the two latter reactions; however, it is useful to begin with a brief review of some pertinent earlier work.

Kannappan[19] observed W-γ interfacial precipitation concurrent with precipitation of a dendritic morphology in the matrix region. This structure was produced in 80W-10Ni-10Fe, 90W-5Ni-5Fe, and 97W-1.5Ni-1.5Fe alloys sintered at 1450°C and 1550°C for various times up to 27 hours and then slow cooled to room temperature. To establish if this precipitate phase was present during liquid phase sintering, the alloy was solution treated at 1300°C and then at 1400°C for 24 hours and quenched to room temperature. The precipitate phase was still present after solution treating at 1300°C but no trace of it was observed after heat treatment at 1400°C. It was concluded that under sintering conditions only two phases, tungsten and liquid, existed and that the slow cool from the sintering temperature allowed the third phase to form. Powder x-ray diffraction results from this multiphase alloy could not be completely interpreted, and consequently, the structure of this third phase was not determined but was said to be "complex". Electron microprobe analysis yielded a precipitate composition of 75W-10Ni-15Fe.

W-γ interphase boundary precipitation was also observed by Edmonds and Jones[20] after furnace cooling a 90W-5Ni-5Fe alloy from the sintering temperature of 1450°C. Scanning and transmission electron microscopy showed that the precipitates exist as platelets ~0.5 μm in length. Thin foil wavelength dispersive x-ray spectrometry showed the precipitate composition to be 78W-10Ni-12Fe ($\pm$2 wt%) - in good agreement with the results of Kannappan.[19] X-ray diffraction was also utilized in order to identify further the interfacial precipitate. As there was reasonable agreement between the tungsten concentrations and the measured d-spacings obtained in this study and those observed by Walsh and Donachie[23] for the intermetallic compound NiW (~ 75 wt%W), the authors tentatively concluded that this precipitate was an intermetallic phase of the form (Ni,Fe)W - an isomorph of NiW. It should be noted that after this alloy was given a heat treatment of 1000 °C and water quenched, the charpy impact energy increased dramatically and the fracture surfaces no longer showed such extensive interfacial separation and no accompanying interphase boundary precipitation was detectable. Instead, the fractional mode exhibited predominantly smooth W-W intergranular separation accompanied by more ductile rupture of the surrounding matrix. Thus, it also appeared that this suspected intermetallic precipitation could be removed by solution treatment, according to the Ni-W phase diagram, with a corresponding improvement in toughness of the heavy alloy.

Henig et al.[11] have also observed interphase boundary precipitation in a 90W-7Ni-3Fe alloy heat treated at $\leq$ 1000° C. They have identified it as an intermetallic compound of the form (Ni,Fe)W, isomorphous with NiW, in agreement with Edmonds and Jones[20]. Discontinuous precipitation

of tungsten was also observed in the matrix upon certain heat treatments in the 800-1000 °C temperature range. After a further 300 hours at temperature, the (Ni,Fe)W intermetallic was seen to form from this precipitated tungsten. This work also included phase equilibria research on the Fe-W binary system. A new intermetallic compound, FeW, was identified and is thought to form peritectoidally from the μ-phase (Fe_7W_6) and tungsten at approximately 1060°C. X-ray diffraction data from this phase was almost identical to that from NiW. As NiW, FeW, and (Ni,Fe)W were all thought to be isomorphous (orthorhombic structure, a_o = 0.776 nm, b_o = 1.248 nm, c_o = 0.710 nm)[23] the authors suggested a modified Ni-Fe-W ternary phase diagram incorporating the (Ni,Fe)W intermetallic with complete iron and nickel miscibility.

Muddle[1] has also recently obtained some interesting results concerning W-γ interphase precipitation in a 91W-4.5Ni-4.5Fe alloy. Numerous selected area and convergent beam electron diffraction patterns were found to be consistent with the precipitate having an $Fd\bar{3}m$ (227) space group with lattice parameter, a_o = 1.092 $\pm$ 0.005 nm. Thin foil energy dispersive x-ray spectrometry showed the concentration of the Z > 11 elements to be, 78.25W-8.95Ni-12.80Fe - in good agreement with previous results.[19,20] Additionally, scanning auger electron spectroscopy data from the precipitate on a fracture surface showed a significant carbon peak - even after prolonged sputtering. The form of the peak (i.e., the presence of two minor peaks at the low energy side of the principal peak) suggested that the carbon was in the form of a carbide rather than a surface deposit. As both the ternary systems Ni-W-C and Fe-W-C have eta-carbides of the form Ni_6W_6C[24] and Fe_6W_6C,[25,26,27] both with $Fd\bar{3}m$ structure and $a_o \simeq$ 1.09 nm, it was

concluded that the interfacial precipitate is an eta-carbide of the form $(Ni,Fe)_6W_6C$ and not an intermetallic compound. In a related study, Muddle and Edmonds[21] observed Widmanstätten laths of eta-carbide within the matrix region in an appropriately heat treated 90W-5.2Ni-4.8Fe alloy which contained 0.014 wt % carbon. A concurrent discontinuous precipitation reaction of tungsten was also found to occur within the matrix region that is believed to be in competition with the eta-carbide precipitation for tungsten.

2. Experimental Procedures

A preliminary study of a commercially produced tungsten heavy alloy, of nominal composition 90W-5Ni-5Fe, provided the impetus for specially fabricating and investigating two Ni-Fe-W alloys. They were designed to simulate the γ-phase matrix of the 90W-5Ni-5Fe alloy which has a composition that was measured by electron microprobe analysis to be 41.4Ni-39.4Fe-19.2W ($\pm$ 0.3 wt %) in the as-supplied material and 39.5Ni-39.2Fe-21.3W ($\pm$ 0.3 wt %) after a 1 hour solution treatment at 1350°C. The matrix-composition alloys were produced by first mixing elemental powders in a rotating mixing drum. Alloy A was subsequently arc-melted in argon to form the Ni-Fe-W ingot directly. Alternatively, the alloy B powder was hydrostatically compressed into a green compact and sintered in a dry hydrogen atmosphere at 1000°C for 2 hours prior to arc-melting. The ingots were homogenized at 1390°C (alloy A) and 1150°C (alloy B) for 50 hours in argon and 10^{-6} torr vacuum, respectively. Table 1 lists the resulting compositions of the matrix-composition alloys along with that of the 90W-5Ni-5Fe heavy alloy. After surface cleaning by grinding, both ingots were swaged to 3mm rod with intermediate anneals at 1350°C for 1 hour after approximately every 50% reduction in area. Alloy A was given a final anneal at 1350°C

for 1 hour, whereas alloy B was given a final anneal at 1350°C for 10 hours. All materials were heat treated in sealed silica tubes under an argon atmosphere, and termination was accomplished by breaking the encapsulating tube into water at ambient temperature.

Slices were cut from 3 mm rods of the materials to be examined. Discs from the heavy alloy were ground to 100 μm thickness, whereas those from the matrix-composition alloys were ground to $\leq$ 50 μm to minimize the deleterious image distortions that a highly magnetic foil produces in the transmission electron microscope. Specimens were electrochemically thinned using a Fischione twin-jet electropolishing unit in an electrolyte of 2% hydroflouric acid, 5% lactic acid, 8% sulfuric acid and 85% methanol. The polishing conditions for heavy alloy specimens were maintained at -30°C, 55Vdc and 95 mA whereas those of the matrix-composition alloys were kept at -35°C, 15Vdc and 18 mA. The majority of transmission electron microscopy was performed at 1000kV to enable increased electron penetration; however, analytical electron microscopy was performed on standard 100kV and 200kV machines. Powder x-ray diffraction of extracted precipitates was accomplished using a Stoe Guinier camera and a Philips diffractometer both using monochromated Cu Kα radiation. Microanalytical data were also obtained using a Cameca Camebax electron microprobe and a Cambridge Mass Spectrometry laser induced ion mass analyzer.

3. Experimental Results

3.1 Matrix Precipitation

Both the 90W-5Ni-5Fe heavy alloy (Fig. 1) and matrix-composition alloy A were examined to establish the nature of the precipitation occurring within the γ-phase matrix. After manufacture, the matrix-composition alloy

was essentially single phase but did contain dispersed inclusions. The inclusions were found to contain a substantial amount of titanium and due to the nature of alloy manufacture, are thought to be complex oxides.

3.1.1. 90W-5Ni-5Fe Heavy Alloy

Transmission electron microscopy revealed a discontinuous precipitation reaction occurring within the matrix region of the heavy alloy when the alloy was subjected to solution treatment at 1350° C for 1 hour, quenched, and subsequently aged at 750-850°C for 100 hours (Fig. 2). This reaction could also be observed in the light microscope - although the reaction product lamellae could not be properly resolved. Prior solution treatment at 1350° C followed by water quenching was essential as simply annealing for 100 hours at 800° C failed to induce discontinuous precipitation. For isochronal heat treatments (t=100 hours) the discontinuous reaction was only observed after solution treating and annealing in the temperature range 750-850° C. Specimens annealed at $\leq$ 650° C or $\geq$ 950°C for 100 hours did not show evidence of precipitation. For annealing at 850° C, precipitation could be observed after 5 hours, but no precipitation was observed after solution treating and annealing at 950°C for 200 hours. Annealing times longer than 100 hours were not attempted at lower temperatures (i.e., $\leq$ 650°C).

Selected area electron diffraction patterns obtained using high voltage electron microscopy consistently showed the identity of the lamellae to be tungsten and γ-phase (Fig. 3). Although the characteristic boundary of the cellular reaction was observed, it was not possible to establish at which microstructural feature the reaction had nucleated. Another important feature that is not shown in these micrographs is the limited

extent of the reaction. Transformed regions were observed only sporadically throughout the alloy and were isolated from one another.

3.1.2. Matrix-Composition Alloy A (40.1Ni-41.1Fe-18.8W)

The fabrication of this alloy included solution treating at 1350° C for 1 hour. Figure 4 shows a series of optical micrographs of specimens aged for 100 hours at temperatures from 750-1250° C at 100° C intervals. The specimens annealed at 750-950° C show a morphology typical of a discontinuous precipitation reaction product. In specimens aged for shorter time, discontinuous precipitation can clearly be seen to nucleate at the grain boundaries and grow into one or both adjacent grains (Fig. 5). As the aging temperature was raised above 950°C the morphology was observed to progress from lamellar to predominantly Widmanstätten form, and finally to grain boundary precipitation at the highest aging temperature of 1250° C.

The precipitate morphology is shown at higher magnification in Figure 6. After heat treating at the lower temperature of 750° C for 100 hours the morphology is essentially lamellar, whereas following aging at 850° C for 100 hours various morphologies can be observed (Fig. 6). Clearly, discontinuous precipitation is present, but the tungsten lamellae appear to be broken up in some areas. In other regions, a Widmanstätten morphology is observed. Aging at the higher temperature of 1050° C produced predominantly Widmanstätten precipitation with a decreased number density and larger size (Fig. 7(a)). At still higher aging temperatures (i.e., 1250°C) precipitation is observed almost exclusively on the grain boundaries. Selected area electron diffraction showed the precipitates to be tungsten - regardless of their morphology. This was subsequently verified by x-ray

diffraction data obtained from powder of the precipitate phase that had been electrochemically extracted from samples aged at various temperatures.

3.2. Interfacial Precipitation

The 90W-5Ni-5Fe heavy alloy and matrix-composition alloy B were studied to elucidate the nature of the W-γ interphase precipitation occurring in the heavy alloy. This matrix-composition alloy was intended to be a single phase simulation of the γ-phase in the solution treated 90W-5Ni-5Fe alloy; however, insoluble precipitates (not oxides) were observed after manufacture. Even after a subsequent treatment at 1390°C for 20 hours, dispersed particles ($\sim$3 μm diameter) of this second phase were still observed. It will be shown that these precipitates bear a crystallographic similarity with the interfacial precipitation observed in the 90W-5Ni-5Fe alloy, and therefore it is appropriate to present the analyses of both consecutively.

3.2.1. 90W-5Ni-5Fe Heavy Alloy

Precipitation was observed at the W-γ interphase boundaries in the heavy alloy occurring concurrently with the discontinuous precipitation described earlier (i.e., after solution treating at 1350°C for 1 hour, quenching, and subsequently annealing at 750-850°C for 100 hours) (Fig. 8). When the alloy was solution treated and annealed at a lower temperature (650°C for 100 hours) or a higher temperature (950°C for 200 hours), no interphase precipitation was observed. The size of the precipitates was $\leq$ 0.4 μm in thickness making them observable only by electron microscopy. Additionally, the reaction was found to be very sporadic and nonuniform, in a manner similar to the discontinuous precipitation reaction. However, there did not appear to be any association between the two reactions - a given region usually exhibited one or the other, or neither morphology.

This same phase was also observed at γ-γ grain boundaries in material heat treated as described above. This morphology was very infrequently observed as there are relatively few γ-γ grain boundaries due to the large γ-phase grain size and only a low percentage of them showed any precipitation. An interface appears to be a prerequisite for the nucleation of this phase in this particular heavy alloy.

Numerous selected area diffraction patterns were obtained from interfacial precipitates located at both W-γ and γ-γ boundaries and all could be indexed consistently with a face-centered cubic Bravais lattice. Using the W-phase as an internal standard (assuming a_0(W-phase)=a_0(tungsten)=0.3165 nm), the lattice parameter of the precipitate phase was found to be, a_0 = 1.096 $\pm$ 0.004 nm.

3.2.2. Matrix-Composition Alloy B (38.5Ni-40Fe-21.5W)

Figure 9 shows a typical transmission electron micrograph of the undissolved precipitate in this alloy. All selected area diffraction patterns obtained were consistent with the precipitate having an f.c.c. Bravais lattice. As there was no internal standard in these specimens, it was not possible to measure accurately the lattice parameter using electron diffraction - although it was estimated to be, a_0 = 1.1 nm.

Convergent beam electron diffraction (CBD) was utilized to ascertain the point group of the precipitate. An appropriate condenser lens current and aperture were chosen that would allow the diffraction discs to overlap - thereby making the high order Laue zone (HOLZ) rings more uniform. Figure 10 shows [111] and [110] zone axes CBD patterns obtained from the precipitate in this manner. Unfortunately, it was not possible to obtain the HOLZ lines in the forward scattered beam (even after decreasing the convergence

angle). Nevertheless, certain symmetries are visible in both patterns. Taking the [111] pattern first, it can be seen that the apparent whole pattern symmetry+ is 3m. Utilizing the tables of Buxton et al.[28], the only possible diffraction groups are; 3m, $3ml_R$ and 6_Rmm_R. Since we know that the crystal is cubic we can restrict ourselves to the five cubic point groups; $m\bar{3}m$, $4\bar{3}m$, 432, $m\bar{3}$ and 23; however, only the point groups $m\bar{3}m$ and $4\bar{3}m$ could be consistent with the three possible diffraction groups. Turning now to the [110] pattern, which has whole pattern symmetry of 2mm, the possible diffraction groups are; 2mm, $2mml_R$ and 4_Rmm_R. From the tables[28] this is quickly narrowed down to diffraction group $2mml_R$, which corresponds to the $m\bar{3}m$ point group. Thus, it is concluded that the point group of the unknown phase in the matrix-composition alloy B is $m\bar{3}m$.

Powder x-ray diffraction of the extracted precipitate phase was accomplished using both a Guinier camera and a diffractometer. The observed reflections can be indexed according to a face-centered cubic Bravais lattice with lattice parameter, $a_0 = 1.1165 \pm 0.0005$ nm (Table II). Since the point group is $m\bar{3}m$ there are ten possible space groups, numbers 221-230; however, numbers 221-224, 229 and 230 can be ruled out immediately as they are simple and body-centered cubic structures. Table III shows the reflection conditions of the remaining possible space groups; $Fm\bar{3}m$ (225), $Fm\bar{3}c$ (226), $Fd\bar{3}m$ (227) and $Fd\bar{3}c$ (228). It can be seen tht the conditions for $Fm\bar{3}c$ and $Fd\bar{3}c$ are not consistent with the x-ray data. Both these space groups disallow {hhl} type reflections where h and l are both odd whereas many of these reflections are in fact observed (e.g., {111}, {331},

+Apparent whole pattern symmetry refers to the entire pattern symmetry except for the direct beam, but because the direct beam always contains equal or more symmetry elements than the whole pattern[29], the apparent whole pattern symmetry is the same as the whole pattern symmetry.

{333}/{511}, etc.). There is not such an obvious difference between space groups $Fm\bar{3}m$ and $Fd\bar{3}m$ when compared to the experimentally observed reflections. There are many permitted reflections for both that have not been detected but this alone does not allow an unambiguous determination of the space group. However, one important difference between the two is that the {200} type reflections are not permitted for $Fd\bar{3}m$ nor are they observed experimentally. Additionally, the {200} type reflections are just barely visible in an [001] selected area diffraction pattern (Fig. 9b). Their presence is due to dynamical scattering between Laue zones. Consequently, it appears that the {200} type reflections are indeed kinematically forbidden and the space group of the insoluble precipitate phase is $Fd\bar{3}m$.

Electron microprobe analysis was performed on a polished bulk specimen of matrix-composition alloy B. The analysis showed the average composition of the precipitate phase to be, 76.5W-10.0Ni-13.5Fe (50.2W-20.6Ni-29.2Fe; $\pm$ 0.3 at %). A detailed scan through the energy spectrum to search for x-rays characteristic of additional elements showed no other element to be present in any significant quantity (i.e. $\geq$ 0.1 wt%). Nevertheless, this result was not considered completely reliable as the electron microprobe was thought to be unsuitable for detecting the presence of small quantities of light elements in a high average atomic number compound. Laser induced ion mass analysis (LIMA) was then used to attempt detection of light elements in the precipitate. Basically, LIMA utilizes a short pulse (10 nsec) of focussed laser radiation to vaporize a small region of the sample. Some small percentage of this material is ionized and subsequently identified with a time-of-flight mass spectrometer.[31] Figure 11 shows spectra obtained

from a region with a precipitate and a region of surrounding matrix. A tiny carbon peak and two seemingly spurious peaks on the low atomic mass side of the calcium and sodium peaks are observed in the precipitate spectrum but not in the matrix spectrum. These spurious peaks, unfortunately, remain unexplained, but the carbon peak is thought to be genuine since (a) it is not accompanied by hydrogen from hydrocarbons, and (b) the sodium, potassium and calcium signals are not larger from the precipitate region - thus indicating that the general contamination level is not greater in the region of the precipitate. Because of the low ionization probability of carbon as compared to nickel, iron and tungsten, the LIMA technique is much less carbon-sensitive, and therefore only a relatively small carbon peak is observed. It must also be noted that spectra are obtained from a volume approximately 5 μm diameter and 0.5 μm deep[32] whereas the precipitates are only about 3 μm diameter. Using these values it is easy to see that a typical precipitate would be expected to contribute to no more than about 50% of a "precipitate region" spectrum while the balance is due to the surrounding matrix. For these reasons, an accurate determination of the carbon concentration of the insoluble precipitate was not attempted using this method.

Thin film energy-dispersive specrometry (EDS) was performed using an ultra-thin window x-ray detector in order to obtain quantitative values for the carbon concentration of the precipitate phase. Spectra were obtained from regions of the foil adjacent to the hole that were very thin (< 20nm) by rastering the electron probe over the specimen for acquisition times of 300-500 seconds (Fig. 12). A small amount of contamination was found to have been produced when the analyzed area was viewed at high

magnification. It was assumed that this build-up was nearly the same in all analyzed regions and was broadly accounted for in the formulation of the K-factors. Approximate K-factors were determined experimentally by using the surrounding matrix as a standard, where the composition was assumed to be the same as the bulk composition (Table 1). A quantification routine that corrected for absorption was used with a reasonable value for the specimen thickness (20nm) and phase density values that were estimated using the electron microprobe and x-ray diffraction data (ρ_{matrix} = 9.6 g-cm^{-3}, $\rho_{precipitate}$ = 14 g-cm^{-3}). The resulting precipitate composition was found to be, 44 at% W - 26 at% Fe - 19 at% Ni - 11 at% C with the error being approximately $\pm$5 at% and $\pm$ 2 at% for the tungsten and carbon, and iron and nickel values, respectively.

4. Discussion

When aged in the 750-850°C temperature range, both the matrix region of the 90W-5Ni-5Fe heavy alloy and matrix-composition alloy A undergo a Type I discontinuous precipitation reaction described by

$$\gamma' \rightarrow W + \gamma$$

where γ' is the tungsten-supersaturated Ni-Fe-W face-centered cubic phase which is being transformed to a more thermodynamically stable mixture of alternating tungsten and γ lamellae. However, there are important morphological and kinetic differences between the reactions in the different alloys. For example, the interlamellar spacing, S, obtained upon transformation during a given heat treatment is not the same in both alloys. S is roughly one micron in matrix-composition alloy A as compared to S 0.5 μm in the transformed matrix regions of the heavy alloy after aging both at 850 °C for 100 hours. This is certainly consistent with the compositional data. The nickel:iron ratio in both matrix-composition alloy

A and the γ-phase of the heavy alloy is approximately unity whereas the tungsten concentration is greater in the γ-phase of the solution treated heavy alloy (21.3 wt % W) than in matrix-composition alloy A (18.8 wt % W). This larger supersaturation of tungsten in the matrix of the heavy alloy suggests that the chemical free energy released per unit volume upon decomposition, ΔG_{chem}, will be greater in the heavy alloy. As the total change in free energy of the transformation (exclusive of interfacial energy) goes as ΔG_{chem},[33] S can be expressed

$$S \propto \Delta G_{chem}^{-1}$$

and a smaller interlamellar spacing would indeed be expected.

The localized and incomplete nature of this reaction in the heavy alloy appears contrary to initial expectation. This can best be understood by considering some of the characteristics of the discontinuous precipitation reaction. Cellular nucleation and growth requires a mobile interface - normally a grain boundary. In this case a W-γ interphase boundary would be unsuitable as this would not actually be nucleation of one phase within another but would instead be a primary tungsten grain developing protrusions (lamellae) into the matrix region. Protrusions from the primary tungsten grains have not been observed in this study. In fact, the tungsten lamellae appear not be in contact with the tungsten grains at all. Muddle and Edmonds[21] have also observed this aspect of the reaction in heavy alloys. Additionally, a mobile grain boundary would have to be created for the reaction to proceed. A more plausible scenario for excess tungsten in solution very near a primary tungsten grain is to precipitate directly onto the tungsten grain as was observed by Kiparisov et al.[22]. The other possible nucleation site would be a γ-γ grain boundary. In this case, the low density of γ-γ grain bounderies may help to explain the irregular

and limited extent of the reaction; however, direct evidence of the nucleation site(s) for this reaction is required before making a final conclusion. It should be noted that other researchers who have observed this reaction[11,19,22], with the exception of Muddle and Edmonds[21], have either not observed its localized nature or have not commented on it. This may be due to their respective alloys containing a significantly larger density of possible nucleation sites (i.e. an alloy with a γ-phase grain size significantly less than that of the tungsten grain size).

At progressively higher aging temperatures ($\geq$ 1050° C) Widmanstätten and grain boundary precipitation of tungsten are observed in matrix-composition alloy A. This is not the case in the matrix region of the heavy alloy where it is believed that aging at 950°C and above has increased the atomic mobility to the extent that excess tungsten precipitates directly onto the primary tungsten crystals. This contrasts with the results of Henig et al.[11] who observed precipitation of tungsten, albeit discontinuously, after aging as high as 1000° C. However, it should be pointed out that this observation was made on a different heavy alloy (90W-7Ni-3Fe) that had been solution treated at the higher temperature of 1400°C.

Because of the low volume fraction and localized nature, the discontinuous precipitation in the matrix region is not believed to affect greatly the mechanical properties of the heavy alloy. This was partially borne out by preliminary testing in which both the yield strength and the ultimate tensile strength were unaltered after solution treating at 1350° C for one hour and subsequently aging at 850° C for 100 hours. Previous results also support this hypothesis. In particular, Henig et al.[11] have

cited results due to Kang[34] and Yoon[35] which could not determine any influence on heavy alloy mechanical properties by the presence of a cellular precipitate morphology in the matrix region.

Turning now to the insoluble precipitates in matrix-composition alloy B, it is apparent that they are carbides with an $Fd\bar{3}m$ space group that contain nickel, iron and tungsten. The existence of eta-carbides with this structure in both Ni-W-C and Fe-W-C ternary systems has been mentioned previously. They typically occur in two forms, M_6C and $M_{12}C$ (M=NiFe, and W) in both systems, and regardless of stoichiometry, are characterized by having an $Fd\bar{3}m$ space group with lattice parameters as listed in Table IV. In fact the lattice parameter of the carbide in matrix-composition alloy B falls between the measured lattice parameters for Ni_2W_4C and Fe_3W_3C. Thus it is concluded that the insoluble precipitate in matrix-composition alloy B is an M_6C eta-carbide. If exact carbon stoichiometry is assumed and then subsequently incorporated with the ratios of the metal element compositions as determined by electron microprobe analysis, the eta-carbide composition would be 75.2W-13.3Fe-9.9Ni-1.6C or, in atomic per cent 43.0W-25.0Fe-17.7Ni-14.3C. These values are consistent with the thin film EDS results and correspond very closely to the $(Ni,Fe)_3W_3C$ stoichiometry typical of the Fe-W-C M_6C eta-carbide, with a nickel:iron atomic ratio of approximately 0.71.

The identity of the W-γ interphase boundary precipitates observed in the 90W-5Ni-5Fe heavy alloy is somewhat less clear. The measured lattice parameter of the f.c.c. phase (a_o = 1.096 $\pm$ 0.004 nm) is very close to that of the Fe_6W_6C eta-carbide. This structure is entirely inconsistent with any of the known phases in the W-Ni-Fe system.[36,37] For these reasons

and by analogy with the $(Ni,Fe)_3W_3C$ carbide found in matrix-composition alloy B, it is believed that this phase is an $M_{12}C$ eta-carbide. Qualitatively, this is consistent with the bulk composition data for the respective materials presented earlier. It would be reasonable to assume that virtually all of the carbon in the heavy alloy would be found in the γ-phase as tungsten has a very limited carbon solubility at the liquid phase sintering temperature (viz., <0.02 at%C at 1450°C)[38]. The volume fraction of the matrix in the 90W-5Ni-5Fe heavy alloy is approximately 0.3[6] which means that a bulk carbon concentration of 0.004 wt % translates to a carbon content of about 0.014 wt % in the γ-phase. This is significantly less carbon than the 0.10 wt % C found in matrix-composition alloy B. It is thus expected that the higher carbon eta-carbide, M_6C, is predominant in the alloy with the higher carbon concentration, and the lower carbon eta-carbide, $M_{12}C$, is predominant in the low carbon concentration heavy alloy. In support of this it should be noted that this behavior is indeed exhibited in both the Ni-W-C and Fe-W-C systems.[24,27]

The interpretation that W-γ interphase boundary precipitates are $M_{12}C$ eta-carbides is consistent with recent results due to Muddle[1], and Muddle and Edmonds[21]. In these studies, eta-carbide precipitates were identified at W-γ interphase boundaries in a commercially produced 91W-4.5Ni-4.5Fe alloy and in an appropriately heat treated experimental 90W-5.2Ni-4.8Fe alloy. Additionally, Widmanstätten laths of $M_{12}C$ were found to have precipitated within the matrix region of the experimental alloy after solution treating at 1350°C and aging at 750-850°C. The alloys used in these studies contained considerably higher amounts of carbon than the tungsten heavy alloy used in the present investigation (Table V). The

absence of $M_{12}C$ Widmanstätten precipitation in the presently studied material is understandable given the lower supersaturation of carbon in the γ-phase and hence the greater propensity for heterogeneous precipitation at the W-γ interphase boundaries and γ-γ grain boundaries.

Certain experimental data from other previous results is also consistent with this interfacial phase being an eta-carbide. For example, the x-ray results reported by Kannappan[19] can be partially rationalized if an eta-carbide with lattice parameter, a_0 = 1.116 nm (i.e., M_6C) is assumed to be present. The additional reflections cannot be explained by assuming the presence of an $M_{12}C$ eta-carbide but could possibly be accounted for if the orthorhombic (Ni,Fe)W intermetallic phase was also present. Another interesting comparison between the present investigation and nearly all previous results is the striking similarity of the reported composition of this additional phase. Excluding carbon, which would not have been detected with the analytical methods that were utilized, the precipitate composition was consistently found to be very near 75W-10Ni-15Fe, regardless of whether the subsequent interpretation concluded it was an $M_{12}C$ eta-carbide,[1] the (Ni,Fe)W intermetallic compound,[11,20] or did not specify the identity.[19]

One possible implication from this last point is that the previous conclusions stating that the additional phase is an intermetallic compound are incorrect. However, this conflicts with the x-ray evidence reported by Edmonds and Jones[20] and Henig, et al.[11]. As mentioned previously, Henig et al.[11] have identified FeW as a new intermetallic compound in the Fe-W binary system, which is isomorphous with orthorhombic NiW, thus furthering the hypothesis that there does exist a (Ni,Fe)W intermetallic compound

that has complete nickel and iron miscibility (Fig. 13). Edmonds and Jones[20] also reported that the interfacial phase dissolved after heat treating the heavy alloy at 1000°C and above, but the $M_{12}C$ eta-carbides are thought to be stable up to approximately 1400°C.[24,39] However, the NiW intermetallic is believed to form peritectoidally below about 1038°C,[23] and (Ni,Fe)W may form at a lower temperature in the ternary alloy. Nevertheless, the present results cannot confirm the existence of the orthorhombic (Ni,Fe)W intermetallic compound in the W-Ni-Fe system. Future experiments in this area should be performed with very pure W-Ni-Fe alloys so that impurity elements will not interfere with the true phase equilibrium determination.

Clearly, the formation of a brittle third phase at the W-γ interphase boundaries should be prevented if adequate heavy alloy ductility is desired. Interphase boundary carbide precipitation can of course be suppressed if the carbon concentration is kept low enough and the thermal processing of the alloy controlled so as to minimize aging in the 750-850°C temperature range. Another approach might be that of microalloying with a strong carbide-forming element (e.g. Nb, Ti or Ta) so as to precipitate carbides uniformly throughout the matrix region and not at the W-γ interphase boundaries. However, further experimental research would be essential to show the viability of this procedure.

5. Conclusions

1) A discontinuous precipitation reaction resulting in alternating tungsten and γ-phase lamellae was found to occur in the matrix region of the 90W-5Ni-5Fe heavy alloy. It was necessary to solution treat at 1350°C for 1 hour and water quench prior to aging in the 750-850°C temperature range to induce this reaction. Even so, the regions transformed in this

manner are sporadic and localized, and the effect on mechanical properties is believed to be negligible.

2) A concurrent heterogeneous precipitation reaction was found to occur sporadically at the W-γ interphase and γ-γ grain boundaries. The precipitate is believed to be an $M_{12}C$ (M = Ni, Fe and W) eta-carbide with lattice parameter, $a_0 = 1.096 \pm 0.004$ nm. This morphology should be avoided if maximum ductility and impact toughness is desired.

3) Two specially manufactured f.c.c. "matrix-composition" alloys have been examined in order to understand better these two precipitation reactions in the heavy alloy. The first was processed so as to induce precipitation of tungsten in various morphologies, and the second was found to contain $(Ni,Fe)_3W_3C$ eta-carbides with lattice parameter, $a_0 = 1.1165 \pm 0.0005$ nm.

Acknowledgments

The authors are grateful to Professor Sir Peter Hirsch, F.R.S. for the provision of laboratory facilities and to Cambridge Mass Spectrometry Ltd. for performing the LIMA microanalysis. We also thank Drs. K.H. Westmacott and U. Dahmen for reviewing the manuscript prior to submission for publication. The bulk of this work has been carried out with the support of the Procurement Executive, Ministry of Defence. One of us (JBP) acknowledges support by the Director, Office of Energy Research, Office of Basic Energy Sciences, Materials Sciences Division of the U.S. Department of Energy under Contract No. DE-AC03-76SF00098 during the completion of this research.

References

1. B.C. Muddle, Metall. Trans. A, 1984, vol. 15A, pp. 1089-1098.

2. J.C. McLennan and C.J. Smithells, J. Sci. Instr., 1935, vol. 12, pp. 159-160.

3. B. Lux, G. Jangg and H. Danninger, The Influence of Chemistry and Various Fabrication Parameters on the Properties of Tungsten Heavy Metals", U.S. Govt. Acc. No. AD-A099799, Feb. 1981, 85 pp.

4. E. Ariel, J. Barta and D. Brandon, Powder Metall. Int., 1973, vol. 5, pp. 126-129.

5. K.S. Churn and R.M. German, Metall. Trans. A, 1984, vol. 15A, pp. 331-338.

6. B.C. Muddle and D.V. Edmonds, Metal Science, 1983, vol. 17, pp. 209-218.

7. K.S. Churn and D.N. Yoon, Powder Metall., 1979, no. 4. pp. 175-178.

8. R.H. Krock and L.A. Shepard, Trans. Metall. Soc. AIME, 1963, vol. 227, pp. 1127-1134.

9. E.J. Votava, Planseeber. Pulvermet., 1973, vol. 21, pp. 79-87.

10. H. Takeuchi, J. Japan Inst. Metals, 1967, vol. 31, pp. 1064-1070.

11. E.-T. Henig, H. Hofmann and G. Petzow, Proc. 10th Plansee Seminar, 1981, vol. 2, ed. H.M. Ortner, pp. 335-359.

12. T.K. Kang, E.-T. Henig and G. Petzow, J. Korean Inst. Metals, 1982, vol. 20, pp. 775-581.

13. Z. Guisen, L. Mingcheng, L. Zhongjie and Y. Shuyan, Acta Metall. Sinica, 1981, vol. 17, pp. 39-43.

14. C. Lea, B.C. Muddle and D.V. Edmonds, Metall. Trans. A, 1983, vol. 14A, pp. 667-677.

15. H. Hofmann and S. Hofmann, Scr. Metall., 1984, vol. 18, pp. 77-80.

16. J.B. Posthill and D.V. Edmonds, Mat. Res. Soc. Symp. Proc., 1984, vol. 21, ed. T. Tsakalakos, pp. 811-816.

17. J.B. Posthill, Proc. 42nd Ann. Meeting EMSA, 1984, ed. G.W. Bailey, pp. 488-489.

18. J.B. Posthill, M.C. Hogwood and D.V. Edmonds, Powder Metall., in press.

19. A. Kannappan, Report No. R70/71, Chalmers University of Technology, Gothenburg, 1971, pp. 47.

20. D.V. Edmonds and P.N. Jones, Metall. Trans. A, 1979, vol. 10A, pp. 289-295.

21. B.C. Muddle and D.V. Edmonds, Acta Metall., in press.

22. S.S. Kiparisov, L.S. Vodop'yanova, Yu. A. Eiduk and Z.S. Isakova, Nauchn. Tr. Vses. Nauch-Issled. Proektn. Inst. Tugo. Met. Tverd. Splanov., 1976, vol. 16, pp. 280-287.

23. J.M. Walsh and M.J. Donachie, Metall. Trans., 1973, vol. 4, pp. 2854-2855.

24. M.-L. Fiedler and H.H. Stadelmaier, Z. Metallkunde, 1975, vol. 66, pp. 402-404.

25. Ya. S. Umanskii and N.T. Chebotarev, Izv. Akad. Nauk SSSR, Ser. Fiz., 1951, vol. 15, pp. 24-38.

26. J. Leciejewicz, J. Less-Common Metals, 1964, vol. 7, pp. 318-320.

27. C.B. Pollock and H.H. Stadelmaier, Metall. Trans., 1970, vol. 1, pp. 767-770.

28. B.F. Buxton, J.A. Eades, J.W. Steeds and G.M. Rackman, Phil. Trans. Roy. Soc., 1976, vol. A281, pp. 171-194.

29. J.W. Steeds and R. Vincent, J. Appl. Cryst., 1983, vol. 16, pp. 317-324.

30. International Tables for X-ray Crystallography, 1983, vol. 4, ed. T. Hahn, pp. 678-701.

31. T. Dingle, B.W. Griffiths, J.C. Ruckman and C.A. Evans, Jr., Microbeam Analysis - 1982, 1982, ed. K.F.J. Heinrich, pp. 365-368.

32. T. Dingle, Cambridge Mass Spectromery Ltd., Cambridge, private communication, 1983.

33. J.W. Christian, The Theory of Transformations in Metals and Alloys Part I, 2nd ed., (1975) Pergamon, Oxford, pp. 507-509.

34. T.K. Kang, Dissertation, Universität Stuttgart, 1981.

35. H.K. Yoon, M.S. Thesis, Korea Adv. Inst. Sci., Seoul, 1980.

36. G.V. Raynor and V.G. Rivlin, Int. Metals Rev., 1981, vol. 26, pp. 213-249.

37. G.V. Raynor and V.G. Rivlin, Int. Metals Rev., 1983, vol. 28, pp. 122-129.

38. H.J. Goldschmidt and J.A. Brand, J. Less-Common Metals, 1963, vol. 5, pp. 181-194.

39. M. Bergström, Mat. Sci. Engr., 1977, vol. 27, pp. 257-269.

TABLE I. Results of bulk chemical analysis in weight per cent for the thirteen elements listed.

Element	95W-5Ni-5Fe (Commerical)	Matrix-Composition Alloy A	Matrix-Composition Alloy B
W	89.7	(18.8)+	21.2 (21.5)+
Ni	4.3	(40.1)+	38.1 (38.5)+
Fe	4.8	(41.1)+	39.7 (40.0)+
C	0.004	0.027	0.10
N	<0.01	<0.001	<0.01
B	<0.0005	nil	0.0014
P	<0.01	nil	<0.01
S	0.003	0.0006	0.005
Ca	0.14	nil	0.02
Na	0.21	nil	0.05
K	0.05	nil	0.02
Si	0.73	nil	0.72
Ti	no analysis	0.011	<0.003

+ - From electron microprobe analysis (± 0.3 wt%).

Line No.	d(nm)	$\{hkl\}_{fcc}$
1	0.6559	111
		200
2	0.3991	220
		311
		222
3	0.2807	400
4	0.2574	331
		420
5	0.2287	422
6	0.2156	333,511
7	0.1979	440
		531
8	0.1866	442,600
9	0.1768	620
		533
10	0.1687	622
		444
11	0.1566	551,711
		640
		642
12	0.1457	553,731
13	0.140 (v. weak)	800
14	0.1366	733
		644,820
15	0.1318	660,822
16	0.1291	555,751
		662
		840
17	0.123 (v. weak)	753,911
		842
18	0.119 (v. weak)	664
		931
		844
19	0.1124	755,771,933
		860,1000
20	0.1096	862,$\overline{10}$20

TABLE II. Experimentally observed x-ray diffraction reflections consistent with a face-centered cubic Bravais lattice with a_o = 1.1165 ± 0.0005 nm.

Space Group (number)	Allowed Reflections (= 2n implied unless otherwise indicated)			
	{hkl}	{0kl}	{hhl}	{00l}
$Fm\bar{3}m$ (225)	h+k,h+l,k+l	k,l	h+l	l
$Fm\bar{3}c$ (226)	h+k,h+l,k+l	k,l	h,l	l
$Fd\bar{3}m$ (227)	h+k,h+l,k+l	k+l=4n k,l	h+l	l=4n
$Fd\bar{3}c$ (228)	h+k,h+l,k+l	k+l=4n k,l	h,l	l=4n

TABLE III. Reflection conditions for the face-centered cubic space groups of $m\bar{3}m$ point group (after reference 30).

Eta-carbide	a_0(nm)	Reference
Ni_6W_6C	1.0900 ± 0.0004	24
Fe_6W_6C	1.0957 ± 0.0001	27
Ni_2W_4C	1.1242 ± 0.0020	24
Fe_3W_3C	1.1124 ± 0.0020	27
$M_{12}C$(M=Ni,Fe,W)	1.096 ± 0.004	(in heavy alloy)
$(Ni,Fe)_3W_3C$	1.1165 ± 0.0005	(in alloy B)

TABLE IV. Lattice parameters of the eta-carbides occurring in the Ni-W-C and Fe-W-C systems with those measured in the present work. The large error associated with the M_6C carbides is thought to be due to their large range of stoichiometry.

Alloy (nominal composition)	Bulk carbon concentration (wt%)	Approximate Carbon concentration in the γ-phase (wt%)	Observed carbide Morphology	Thermal treatment	Reference
91W-4.5Ni-4.5Fe (commercial)	0.045	0.22	Extensive interphase boundary $M_{12}C$	Furnance cool from sintering temperature	1,21
90W-5.2Ni-4.8Fe (experimental)	0.014	0.06	Sporadic Widmanstätten and interphase boundary $M_{12}C$	S.T. 1350°C, 1 hr. and 750-950°C, 10 + hrs.	21
90W-5Ni-5Fe (commercial)	0.004	0.014	Sporadic interphase boundary $M_{12}C$	S.T. 1350°C, 1 hr. and 750-850°C, 100 hrs.	this work
21.2W-38.1Ni-39.7Fe (experimental)	0.10*	-	Uniform distribution of ~3μm diameter M_6C	Upon manufacture final anneal, 1390°C, 20 hrs.	this work

TABLE V. Comparison of the W-Ni-Fe alloys in which the presence of an eta-carbide has been experimentally established.

(*- this high carbon concentration is believed to be due to contamination occurring during the hydrostatic pressing of the blended metal powder).

Figure Captions

Fig. 1. Optical micrograph of the commercially supplied 90W-5Ni-5Fe heavy alloy.

Fig. 2. Discontinuous precipitation in the matrix region of the heavy alloy (a) TEM, solution treated at 1350°C for 1 hour (S.T.) and aged at 750 °C for 100 hours, (b) TEM, S.T. and aged at 850°C for 100 hours; (c) optical, S.T. and aged at 850°C for 100 hours; (d) optical, S.T. and aged at 850°C for 20 hours.

Fig. 3. TEM micrographs identifying the lamellae as W and γ (a) bright field, (b) dark field using a tungsten reflection.

Fig. 4. Precipitate morphology as a function of aging temperature (t = 100 hours) for matrix-composition alloy A (a) 750°C, (b) 850°C, (c) 950°C, (d) 1050°C, (e) 1150°C, (f) 1250°C.

Fig. 5. Discontinuous precipitation initiating at grain boundaries in matrix-composition alloy A after 750°C for 10 hours (note the double seam morphology).

Fig. 6. Transmission electron micrographs of matrix-composition alloy A showing different precipitate morphologies after aging at 850°C for 100 hours (a)-(c) different areas (see text for description).

Fig. 7. Transmission electron micrographs of matrix-composition alloy A showing (a) Widmanstätten morphology, 1050°C for 100 hours; (b) grain boundary allotriomorph, 1250°C for 100 hours.

Fig. 8. Transmission electron micrographs showing interfacial precipitation in the heavy alloy. (a) W-γ boundary, S.T. and aged at 750°C for 100 hours; (b) W-γ boundary, S.T. and aged at 850°C for 100 hours; (c) γ-γ boundary,

S.T. and aged at 750 °C for 100 hours; accompanying f.c.c. selected area diffraction patterns, (d) $\underline{B}=[011]$, (e) $\underline{B}=[\bar{1}13]$, (f) $\underline{B}=[2\bar{3}3]$, (g) $\underline{B}=[\bar{1}35]$, (h) $\underline{B}=[1,7,\overline{12}]$.

Fig. 9. Transmission electron micrograph of the insoluble precipitate in matrix-composition alloy B (a) bright field; accompanying f.c.c. selected area diffraction patterns, (b) $\underline{B}=[001]$ (the {200} type reflections are too weak to be photographically reproduced but are visible on the negative), (c) $\underline{B}=[111]$, (d) $\underline{B}=[235]$, (e) $\underline{B}=[455]$, (f) $\underline{B}=[479]$.

Fig. 10. Convergent beam electron diffraction patterns from the precipitate in matrix-composition alloy B (a) $\underline{B}$ = [111] with 3m whole pattern symmetry, (b) $\underline{B}$ = [110] with 2mm whole pattern symmetry.

Fig. 11. LIMA spectra from matrix-composition alloy B (a) surrounding matrix, (b) precipitate region showing a small carbon peak.

Fig. 12. Representative EDS spectra obtained from matrix-composition alloy (B) (a) surrounding matrix, (b) insoluble precipitate showing significantly more carbon. The labeled peaks were those used for quantification.

Fig. 13. The 800° C isotherm for W-Ni-Fe phase equilibria proposed in reference 11.

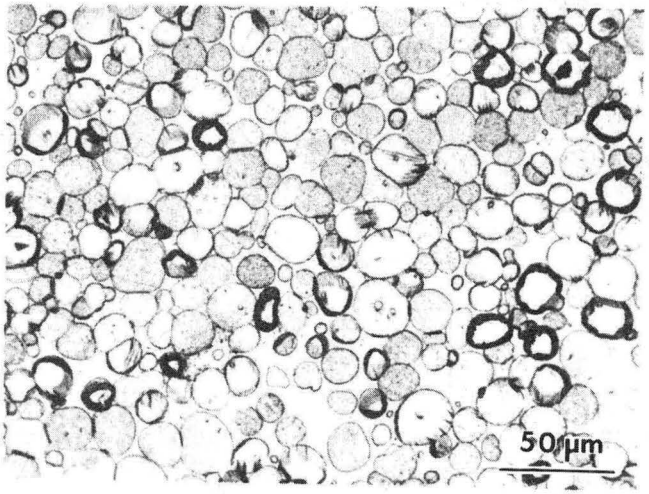

XBB 8510-8734

Fig. 1

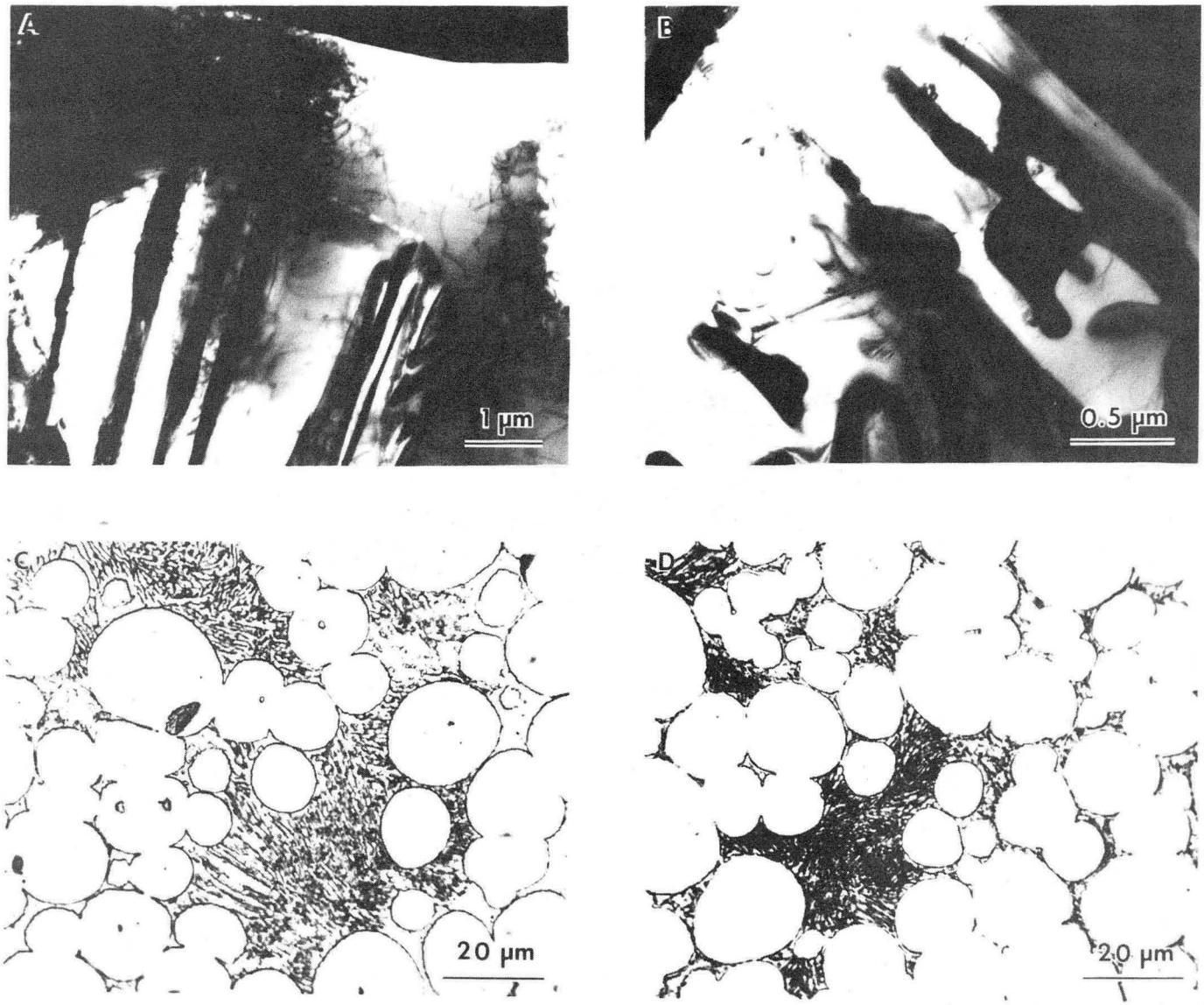

XBB 8510-8742

Fig. 2

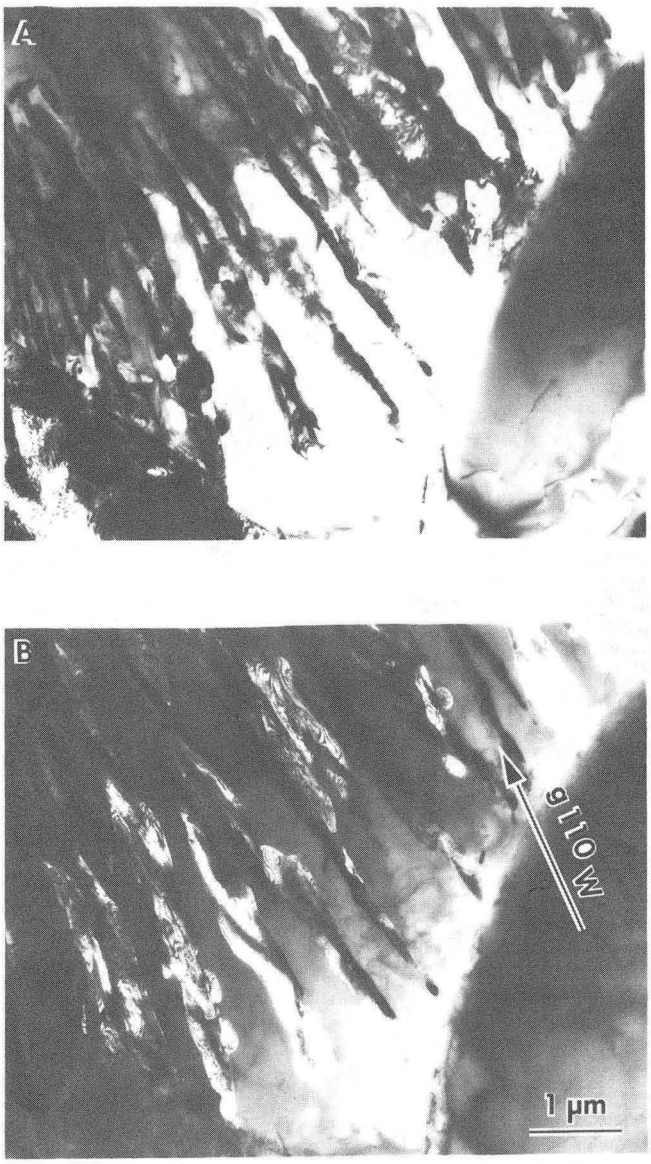

XBB 8510-8741

Fig. 3

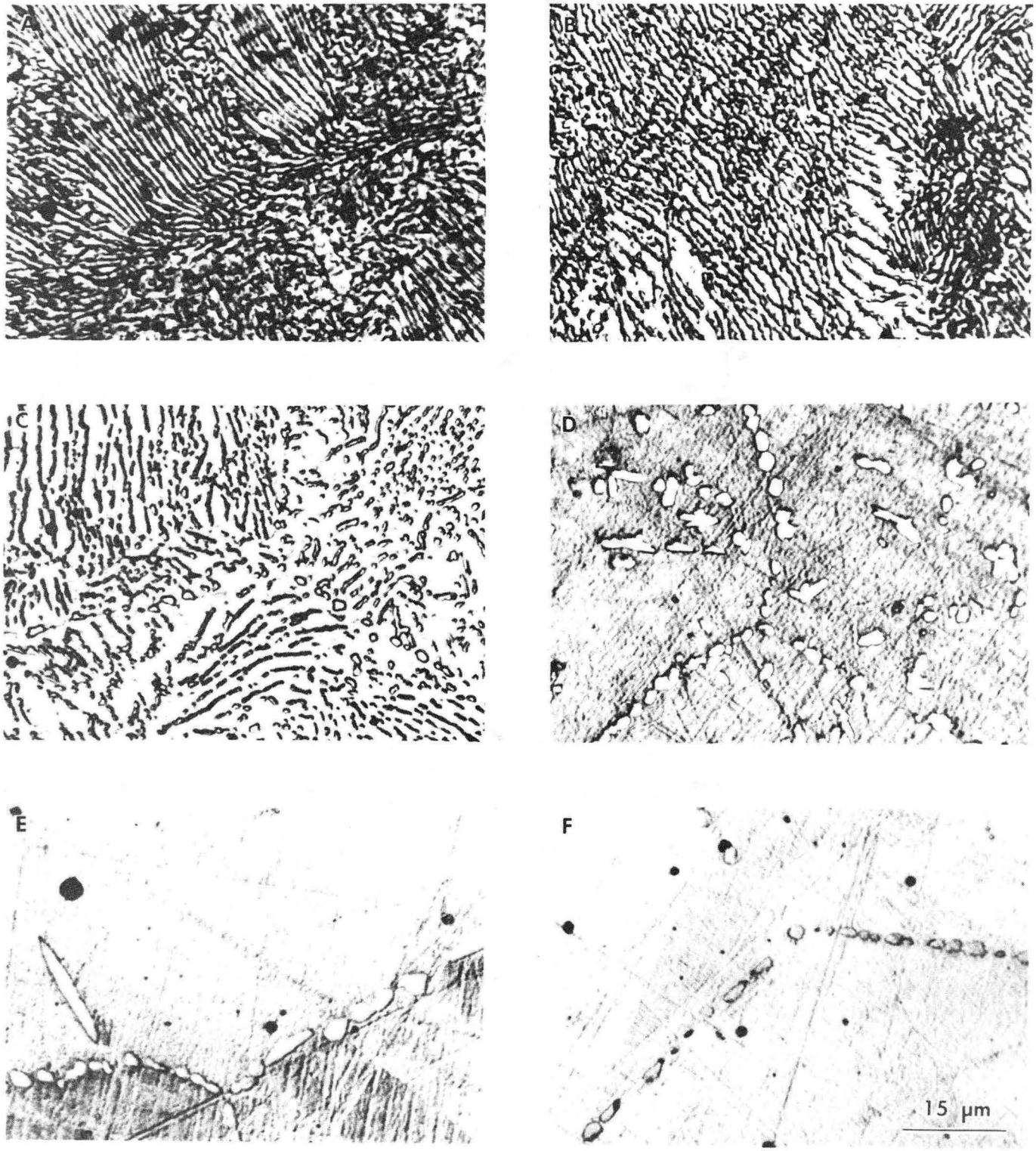

XBB 8510-8735

Fig. 4

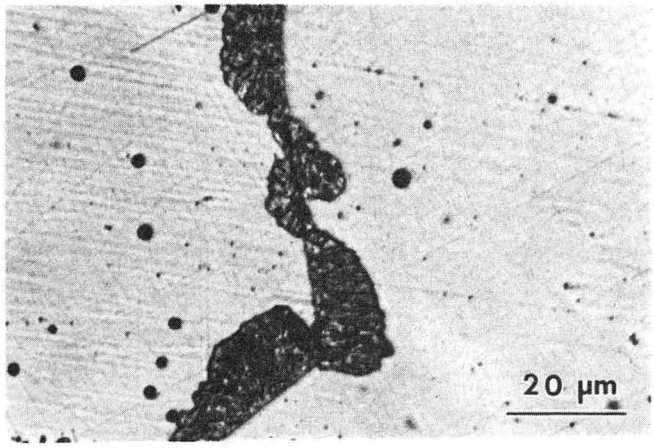

XBB 8510-8733

Fig. 5

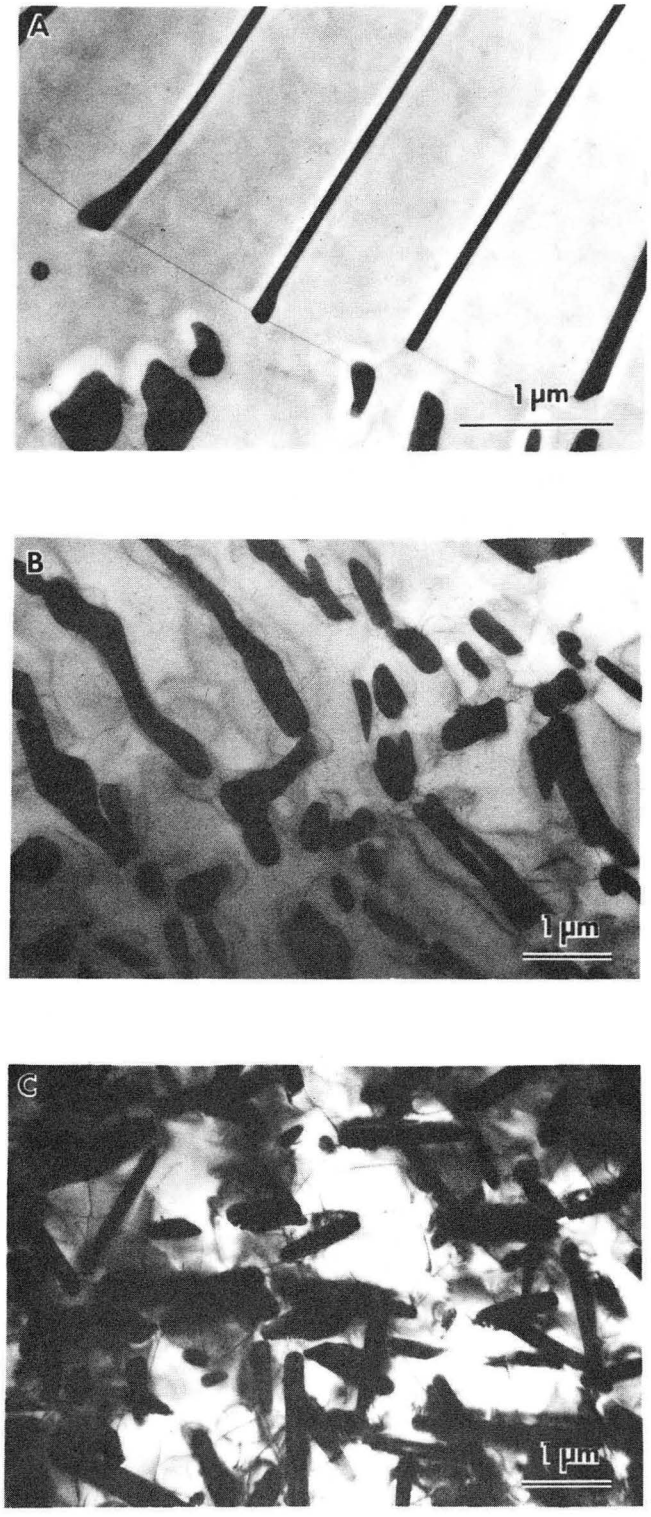

XBB 8510-8740

Fig. 6

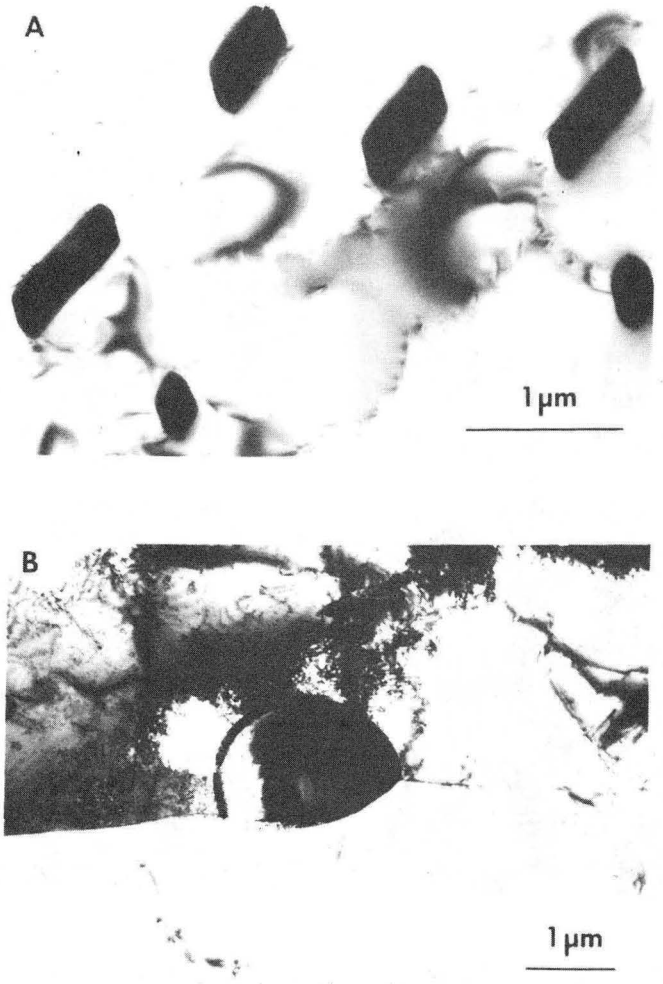

XBB 8510-8739

Fig. 7

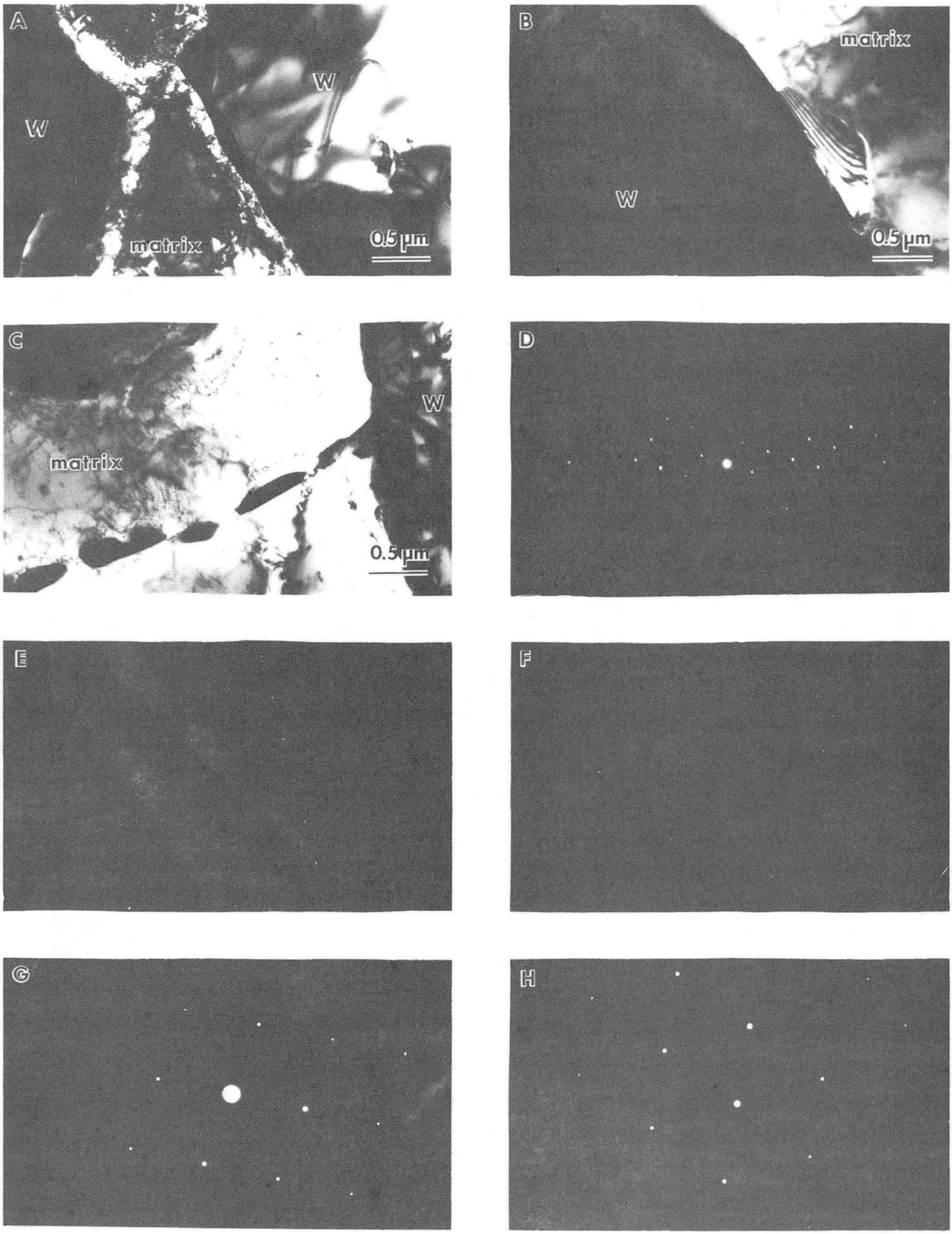

XBB 8510-8738

Fig. 8

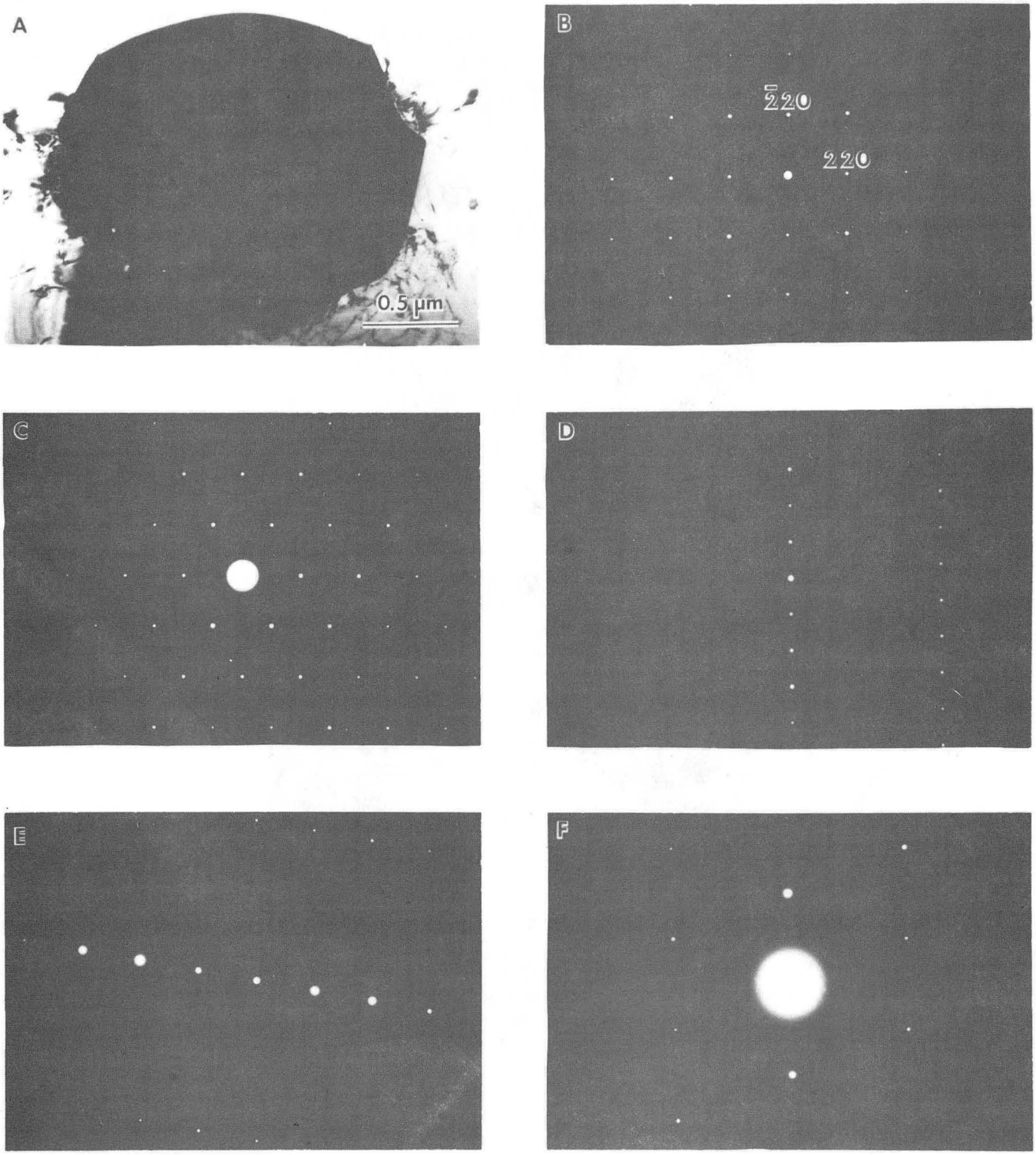

XBB 8510-8737

Fig. 9

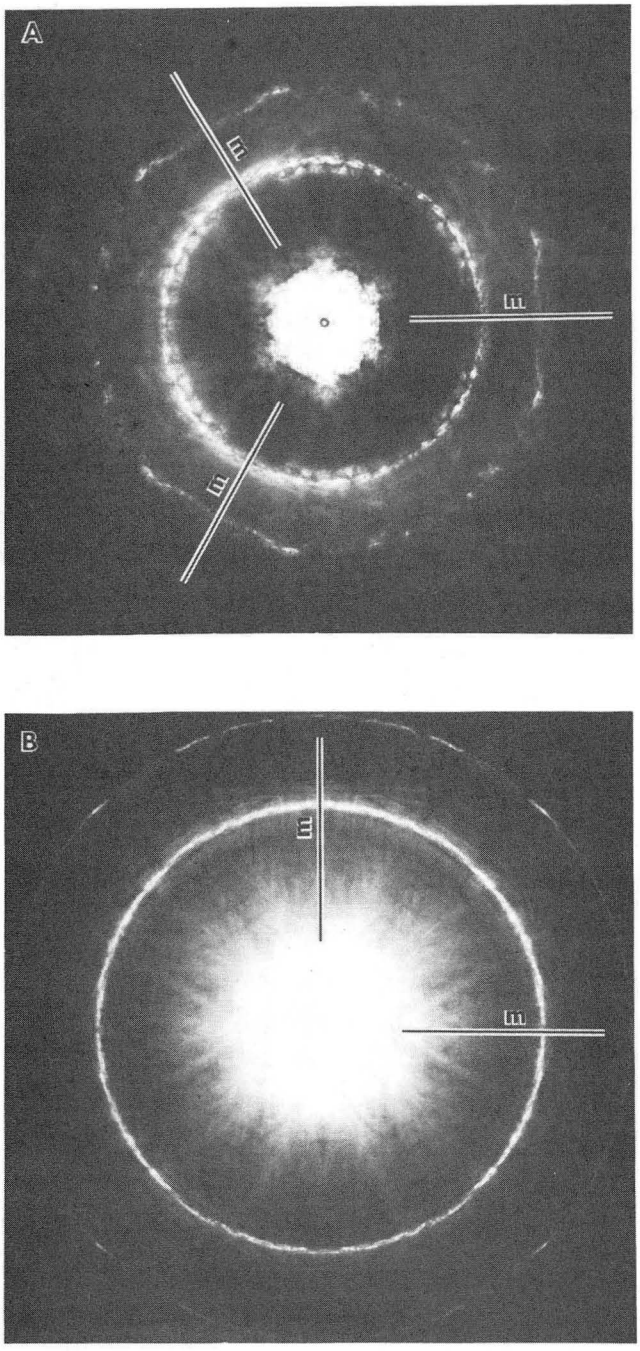

XBB 8510-8736

Fig. 10

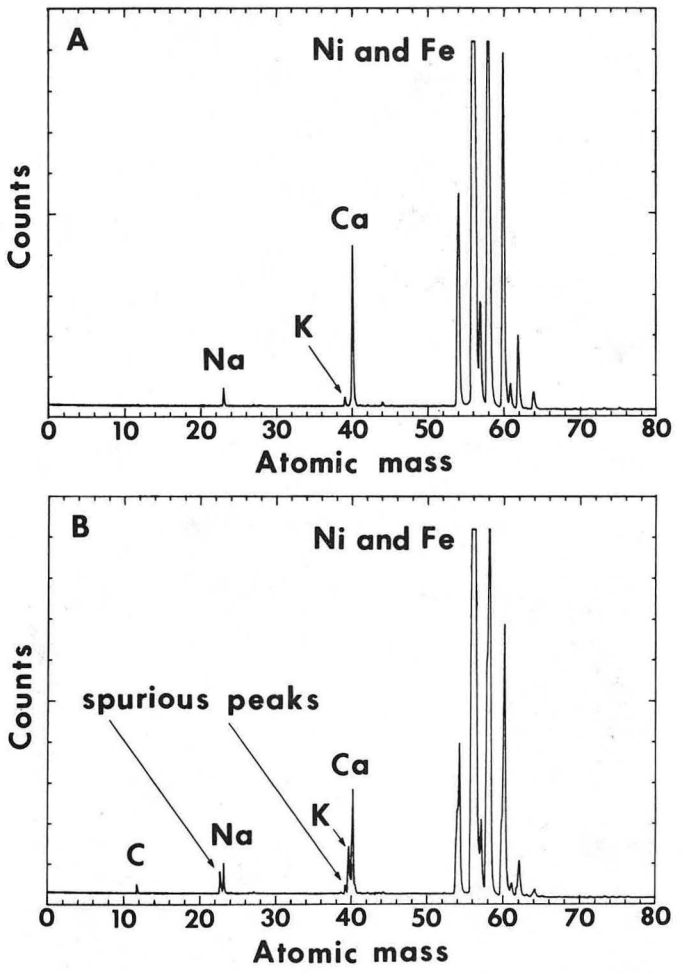

XBL 8511-4502

Fig. 11

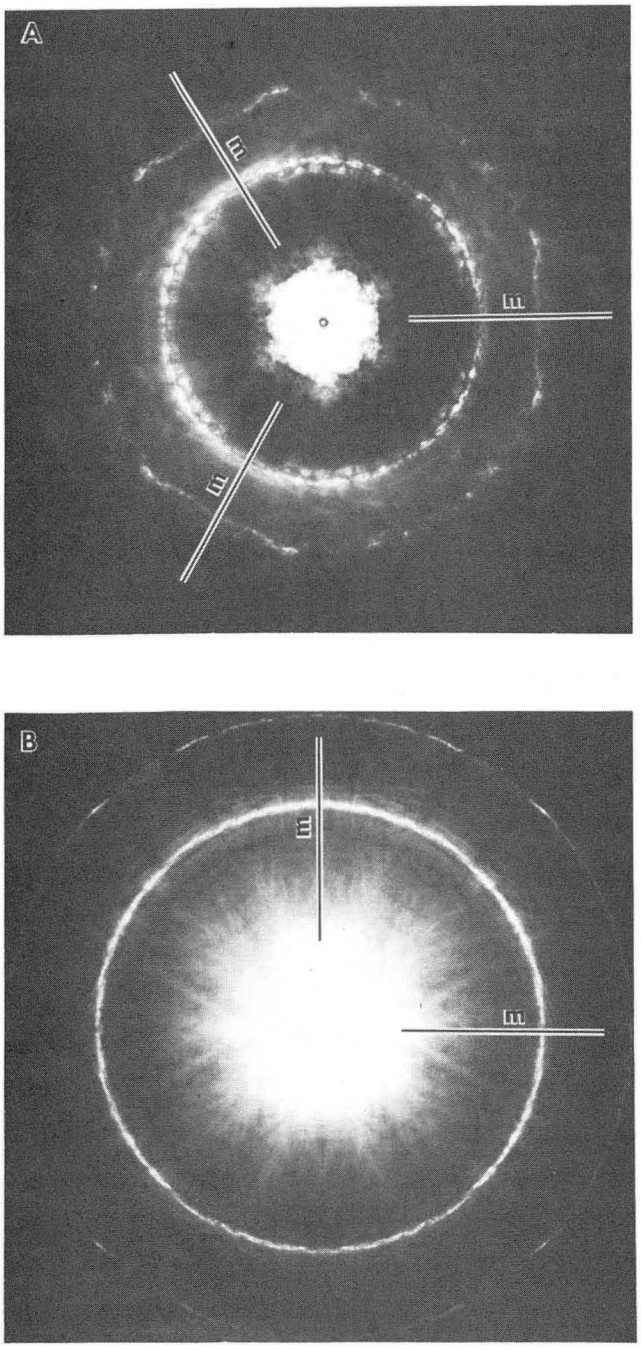

XBB 8510-8736

Fig. 10

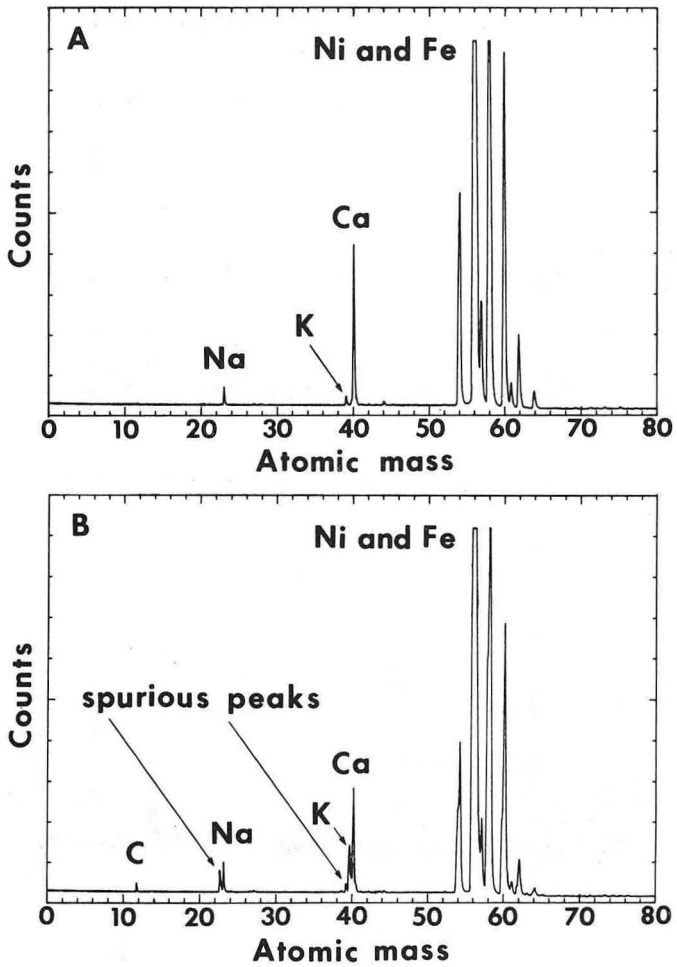

XBL 8511-4502

Fig. 11

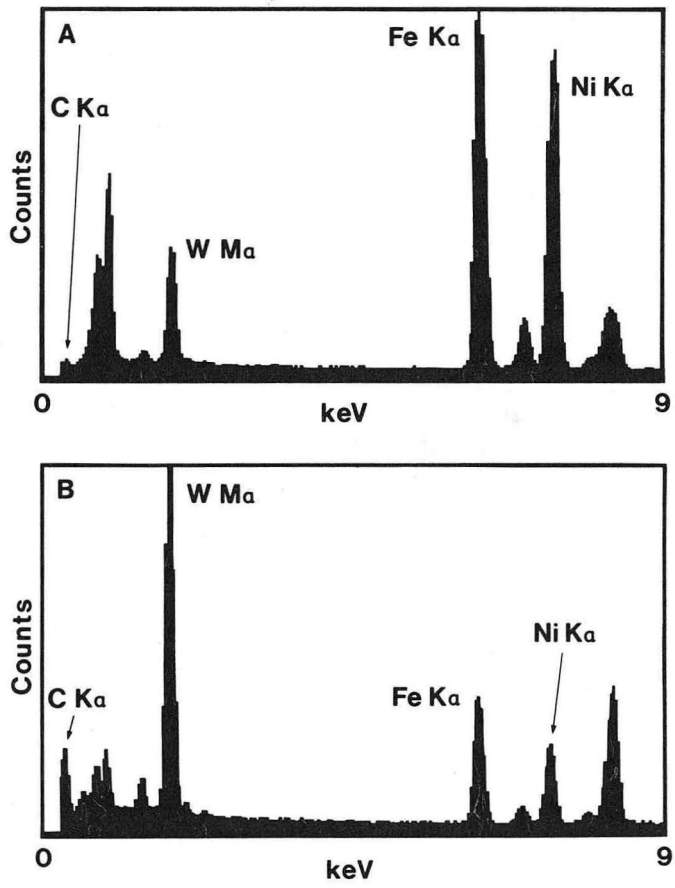

XBL 8511-4504

Fig. 12

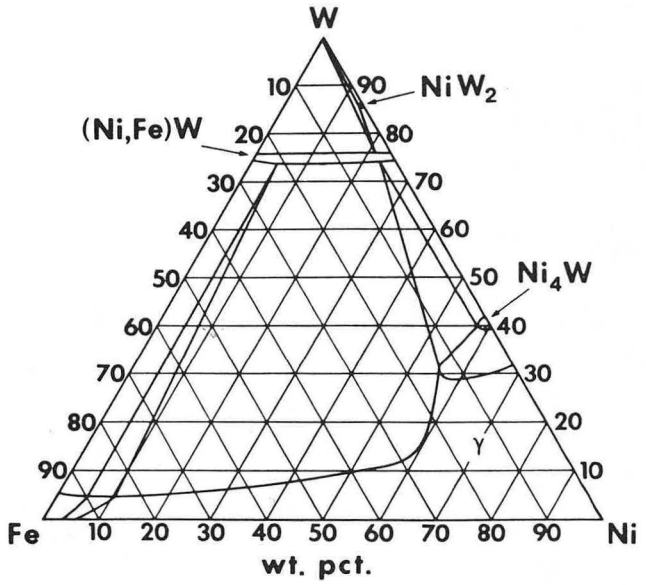

XBL 8511-4503

Fig. 13

This report was done with support from the Department of Energy. Any conclusions or opinions expressed in this report represent solely those of the author(s) and not necessarily those of The Regents of the University of California, the Lawrence Berkeley Laboratory or the Department of Energy.

Reference to a company or product name does not imply approval or recommendation of the product by the University of California or the U.S. Department of Energy to the exclusion of others that may be suitable.

LAWRENCE BERKELEY LABORATORY
TECHNICAL INFORMATION DEPARTMENT
UNIVERSITY OF CALIFORNIA
BERKELEY, CALIFORNIA 94720